



Fermi National Accelerator Laboratory

FERMILAB-Conf-94/016-E

DØ

**Study of Associated Gauge Boson Production at DØ:
W γ Production**

**Anthony L. Spadafora
For the DØ Collaboration**

*SSC Laboratory
2550 Beckleymeade Avenue, Dallas, Texas 75237*

*Fermi National Accelerator Laboratory
P.O. Box 500, Batavia, Illinois 60510*

January 1994

To appear in the Proceedings of the *9th Topical Workshop on Proton-Antiproton Collider Physics*,
Tsukuba, Japan, October 18-22, 1993

Disclaimer

This report was prepared as an account of work sponsored by an agency of the United States Government. Neither the United States Government nor any agency thereof, nor any of their employees, makes any warranty, express or implied, or assumes any legal liability or responsibility for the accuracy, completeness, or usefulness of any information, apparatus, product, or process disclosed, or represents that its use would not infringe privately owned rights. Reference herein to any specific commercial product, process, or service by trade name, trademark, manufacturer, or otherwise, does not necessarily constitute or imply its endorsement, recommendation, or favoring by the United States Government or any agency thereof. The views and opinions of authors expressed herein do not necessarily state or reflect those of the United States Government or any agency thereof.

Study of Associated Gauge Boson Production at DØ: $W\gamma$ Production¹

The DØ Collaboration
Presented by Anthony L. Spadafora
SSC Laboratory
Dallas, TX 75237, USA

Preliminary results are presented from a study of $\bar{p}p \rightarrow W\gamma + X$ at $\sqrt{s} = 1800$ GeV at DØ using data from its recently completed first run at the Fermilab Tevatron Collider. The analysis is performed in both the electron and muon channels. In each channel 10 events are observed, which, after subtracting backgrounds, agrees with the Standard Model expectation. Study of this process is a direct test of the couplings of the $WW\gamma$ vertex. Using a Monte Carlo calculation of the dependence of the number of expected events on these couplings, we set preliminary limits (at the 95% confidence level) on the anomalous couplings of $-2.5 \leq \Delta\kappa \leq 2.7$ ($\lambda = 0$) and $-1.2 \leq \lambda \leq 1.1$ ($\Delta\kappa = 0$).

1. Introduction

As large statistics samples of W and Z bosons become available, it is now becoming feasible to observe vector boson pair production at the Fermilab Tevatron. Restricting consideration to vector boson decays to either electrons or muons, of the various combinations ($WW, ZZ, WZ, W\gamma, Z\gamma$) the two channels involving photons have the largest signals.

The study of the process $\bar{p}p \rightarrow W\gamma + X$ provides a measurement of the $WW\gamma$ vertex, a fundamental coupling in the Standard Model of electroweak interactions. Events of this type can be produced by “ $W\gamma$ production” ($\bar{p}p \rightarrow W\gamma + X$, i.e. W production accompanied by photon emission from an initial state quark or the W boson) or “radiative W decay” ($\bar{p}p \rightarrow W + X \rightarrow e\nu\gamma + X$, i.e. inclusive W production with radiation from a final state charged lepton.) (In all references below, “ $W\gamma$ ” is meant to include both processes.) These events provide a direct test of the couplings of the trilinear $WW\gamma$ vertex, and hence of the W magnetic dipole and electric quadrupole moments. It should be noted that this is the only *direct* test of these fundamental quantities available at current accelerators, as compared to the model-dependent bounds extracted from low-energy phenomena, such as $b \rightarrow s\gamma$.

The trilinear vertex $WW\gamma$ can be described by an effective Lagrangian[1, 2] in which the couplings are represented by κ and λ . (There are additional CP violating terms with other couplings which are not considered here.) These couplings are related to the W boson magnetic dipole (μ_W) and electric quadrupole (Q_W) moments by:

$$\mu_W = \frac{e}{2M_W}(1 + \kappa + \lambda) \quad Q_W = \frac{-e}{M_W^2}(\kappa - \lambda)$$

¹To appear in the Proceedings of the “9th Topical Workshop on $\bar{p}p$ Collider Physics”, Tsukuba, Japan, Oct. 18-22, 1993.

In the Standard Model, at the tree level, $\Delta\kappa = \lambda = 0$ where $\Delta\kappa = \kappa - 1$.

As discussed in Ref. [2], the presence of anomalous (i.e. non Standard Model) couplings results in modification of the kinematic distribution of the final state particles, such as an enhancement of the photon spectrum at high E_T . But, as can be seen in Fig. 1, the cross section itself is also sensitive to the anomalous couplings. In fact, since the amplitudes are linear in $\Delta\kappa$ and λ , the cross section has a quadratic dependence on these quantities. Previous limits on anomalous couplings have been set by CDF[3] using the cross section and by UA2[4] using the cross section as well as fits to the differential spectra of the final state particles.

This paper reports on a preliminary analysis of $W\gamma$ production at $\sqrt{s} = 1800$ GeV at DØ using data from its recently completed first run at the Fermilab Tevatron collider. The analysis has been performed in both the electron ($W \rightarrow e\nu$) and muon ($W \rightarrow \mu\nu$) channels. Preliminary limits on the anomalous couplings are obtained from both channels individually as well as from the combined data sample.

2. Event Selection

The DØ detector is described in detail in Ref. [5], and the aspects relevant to detecting W bosons is reviewed in Ref. [6]. The two elements most relevant to the present analysis are the calorimeter and muon systems. The calorimeter system consists of uranium-liquid argon sampling detectors in a central (CC) and two end (EC) cryo-

stats, with a scintillator tile array in the inter-cryostat regions. The calorimeter provides hermetic coverage in pseudorapidity out to $|\eta| \sim 4$. The energy resolution of the calorimeter has been measured in beam tests[7] to be $15\%/\sqrt{E}$ for electrons (where E is in GeV) and $50\%/\sqrt{E}$ for isolated pions. The calorimeter is read out in towers that subtend 0.1×0.1 in $\eta \times \phi$ and are segmented longitudinally into 4 electromagnetic and 4-5 hadronic layers. In the third EM layer the towers are subdivided transversely into 0.05×0.05 . The muon system consists of magnetized iron toroids with one inner and two outer layers of drift tubes. It has a design momentum resolution of $\delta p/p = 0.2 \oplus 0.01p$ and provides coverage out to $|\eta| \leq 3.3$. The event selection procedure used here is similar to that of the DØ inclusive W analysis described in Ref. [6] but with the requirement of an additional photon.

The Electron Channel:

For the study of $\bar{p}p \rightarrow W\gamma + X$, where the W decays to an electron and a neutrino, we have searched for events with an electron with $E_T \geq 25$ GeV, a photon with $E_T \geq 10$ GeV, and missing transverse energy $\cancel{E}_T \geq 25$ GeV. The electron and neutrino are also required to

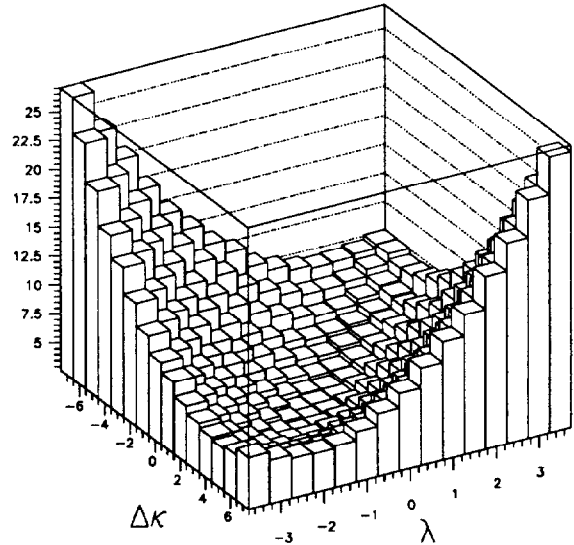


Figure 1: The cross section in pb^{-1} for $\bar{p}p \rightarrow W\gamma + X$ in the electron channel at $\sqrt{s} = 1800$ GeV as a function of $\Delta\kappa$ and λ . The kinematic cuts given in Section 2 are applied in the calculation.

have a transverse mass $M_T \geq 40 \text{ GeV}/c^2$. The events were triggered with the $D\bar{O}$ inclusive W trigger, which requires an electromagnetic cluster with $E_T \geq 20 \text{ GeV}$ and missing transverse energy $\cancel{E}_T \geq 20 \text{ GeV}$. (This trigger also includes a “Main Ring Veto” that disables triggers coincident with the passage of the Main Ring beam through $D\bar{O}$.) The offline kinematic cuts of 25 GeV were chosen to be high enough above the trigger thresholds so that systematic effects in the trigger efficiency are negligible.

The offline electron identification employed here is the standard $D\bar{O}$ algorithm (see Ref. [6] and the references cited therein.) The essential features are the observation of an electromagnetic cluster in the calorimeter with:

- a good quality matching track reconstructed in the central tracking detector (CD)
- the number of calorimeter cells $N_{cells} \geq 20$
- the ratio of energy in the electromagnetic calorimeter layers to that in all layers $EM/TOTAL \geq 0.90$
- isolation $I \leq 0.15$ where isolation is defined as

$$I = \frac{E_{Total}(R < 0.4) - E_{EM}(R < 0.2)}{E_{EM}(R < 0.2)}$$

(R denotes the distance from the shower center in $\Delta\eta \times \Delta\phi$ space.)

- a shower covariance matrix χ^2 cut.

For this analysis the cluster is required to be within the following fiducial volume. In the central calorimeter the cluster must have a “detector” pseudorapidity² of $|\eta| \leq 1.1$ and must be away from the azimuthal cracks between the 32 electromagnetic modules ($\Delta\phi > \pm 0.01$ radians.) In the end calorimeter, a detector pseudorapidity $1.5 \leq |\eta| \leq 2.5$ is required. All reconstructed calorimeter energies are corrected by the energy scale determined from the $Z \rightarrow ee$ mass[6]).

The requirements on the identification of the photon are the same as those on the electron, except that we require that there be no track matching the cluster and the isolation cut is somewhat tighter ($I \leq 0.10$). In addition, we require that the separation between the photon and the electron be $\Delta R_{e\gamma} \geq 0.7$ where $\Delta R_{e\gamma} = \sqrt{\Delta\eta_{e\gamma}^2 + \Delta\phi_{e\gamma}^2}$. This cut[2] suppresses the contribution of the radiative decays and with this minimum separation we are able to reconstruct the electron and photon with no loss of efficiency due to the clusters merging.

Muon Channel:

In this channel we searched for events containing a muon with $P_T \geq 15 \text{ GeV}/c$, a photon with $E_T \geq 10 \text{ GeV}$, and missing transverse energy $\cancel{E}_T \geq 15 \text{ GeV}$. The thresholds for the muon and the \cancel{E}_T are lower than in the electron channel because we used a muon+EM cluster trigger whose rates permitted lower thresholds. The trigger used for this analysis

²i.e. its pseudorapidity calculated as if the particle originated at the nominal detector center along the beam axis ($z = 0$). Unless otherwise noted, pseudorapidity is calculated from the reconstructed event vertex position along the beam axis.

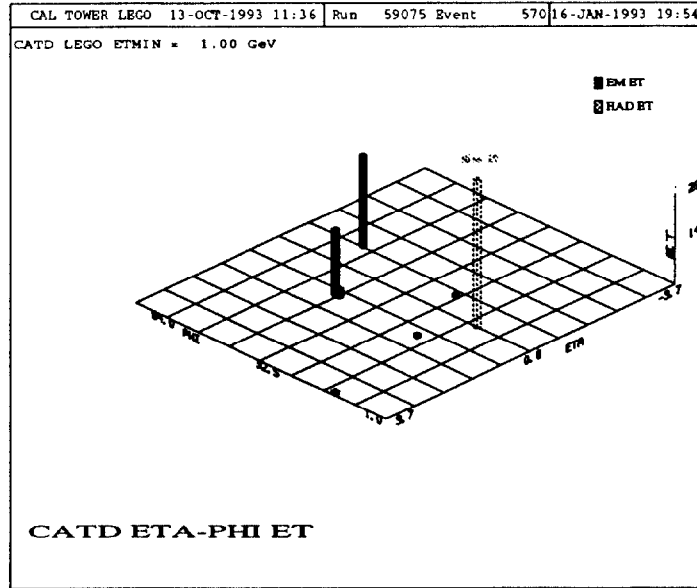


Figure 2: Lego plot of a candidate event in the electron channel.

required an electromagnetic cluster with $E_T \geq 7$ GeV, a muon with $P_T \geq 5$ GeV/c, and had no main ring veto.

The offline muon analysis is essentially the same as that used in the inclusive $W \rightarrow \mu\nu$ analysis[6]. The track stub found in the muon layers is required to have a hit in the inner layer. For an accurate momentum measurement, the muon is required to pass through a minimum length of magnetized iron. It must also have a matching central detector track (with an acceptable impact parameter) as well as a signal in the calorimeter, which is used to calculate a dE/dX correction to the muon momentum. Cosmic ray events were rejected using timing and track impact parameter cuts. The fiducial volume used for this analysis used the central (CF) and end (EF) regions of the DØ wide angle muon system which covers pseudorapidity range $|\eta| \leq 1.7$.

Results:

After applying these event selection procedures to our data sample, which corresponds to a total integrated luminosity of $L_{tot} = 14.9 \pm 1.8$ pb⁻¹ for the electron analysis and 14.4 ± 1.7 pb⁻¹ for the muon analysis, we are left with 10 events in each channel. A lego plot, displaying the deposition of transverse energy in the calorimeter versus η and ϕ , is shown in Fig. 2 for one of the electron channel events. In this figure, the taller of the two dark towers corresponds to an $E_T = 34$ GeV electron, the shorter to an $E_T = 29$ GeV photon, and the tower shown in outline indicates the azimuthal orientation of the 54 GeV of missing transverse energy. The separation between the electron and the photon is $R_{e\gamma} = 2.1$ and the $e-\nu$ transverse mass is $M_T = 84$ GeV/c². This event has no measurable jet activity. Defining jets with a cone algorithm ($R = 0.5$) and requiring a minimum E_T of 15 GeV, we find that of the 10 electron candidate events, 6 have no jets, 3 have 1 jet, and 1 event has 2

jets. The breakdown by jet topology is similar in the muon events. The distributions of the relevant kinematic quantities for the electron channel events are shown in Fig. 3 and for the muon channel events in Fig. 4. The l - ν - γ cluster transverse mass (where $l = e$ or μ), shown in Figs. 3 and 4, is defined as

$$M_T^2(l\gamma; \cancel{E}_T) = \left(\sqrt{M_{l\gamma}^2 + |\mathbf{E}_{T\gamma} + \mathbf{E}_{Tl}|^2} + \cancel{E}_T \right)^2 - |\mathbf{E}_{T\gamma} + \mathbf{E}_{Tl} + \cancel{E}_T|^2$$

where the items in boldface are vector quantities and $M_{l\gamma}^2$ is the invariant mass of the l - γ pair. As discussed in Ref. [2], events with cluster transverse mass less than $90 \text{ GeV}/c^2$ are predominately from final state radiation (“ W radiative decay”) while those greater than $90 \text{ GeV}/c^2$ are from initial state radiation (“ $W\gamma$ production”).

3. Estimation of Background

In the study of a rare process such as $W\gamma$ production, the estimate of the contribution to the observed number of events from background processes is a key step. The major sources of background for $W\gamma$ production are:

1. $W \rightarrow l\nu + \text{jets}$, where a jet is misidentified as a photon
2. $Z\gamma + X$, where the Z decays to ll and one of the leptons is missed by the detector and so contributes \cancel{E}_T
3. $W\gamma$, with $W \rightarrow \tau\nu$ and $\tau \rightarrow l\nu\nu$.
4. $ee + \text{jets}$, where an electron is misidentified as a photon (electron channel only)
5. Cosmic rays (muon channel only)

Our calculation of the number of background events arising from each of these sources is as follows.

We calculate the magnitude of the $W + \text{jets}$ background in each channel by first determining the probability that a jet passes our photon identification criteria, $Prob(\text{jet} \rightarrow \gamma)$, and then multiplying this by the number of jets observed in the inclusive W sample for this channel. The quantity $Prob(\text{jet} \rightarrow \gamma)$ is both detector and algorithm specific; we estimate it by measuring the fraction of jets in samples of QCD dijet or trijet events that pass our photon cuts. The values obtained are $Prob(\text{jet} \rightarrow \gamma) = (0.83 \pm 0.14) \times 10^{-3}$ in the CC and $(1.37 \pm 0.59) \times 10^{-3}$ in the EC. We observe a slight variation of these numbers over the E_T range of the photons in our candidate events, and this is included in the systematic errors quoted. In the inclusive $W \rightarrow e\nu$ sample the number of jets with $E_T \geq 10 \text{ GeV}$ in our CC fiducial volume is 1933 ± 44 and in the EC the number is 1200 ± 35 . Combining these numbers with $Prob(\text{jet} \rightarrow \gamma)$, we obtain $N_{jets}(e) = 3.2 \pm 1.6$ background events for the electron channel. In the muon channel, the number of jets in the inclusive $W \rightarrow \mu\nu$ sample is 1081 ± 106 in the CC and 430 ± 51 in the EC. These numbers result in a background contribution of $N_{jets}(\mu) = 1.5 \pm 0.3$ events.

The next two sources of background contribute amounts proportional to the signal: $N_Z = f_Z N_{signal}$ for the $Z\gamma$ background, and $N_\tau = f_\tau N_{signal}$ for the $W\gamma, W \rightarrow \tau\nu$ background. We write the observed number of events as a sum of signal and backgrounds:

$$N_{obs} = N_{signal} + (f_Z + f_\tau)N_{signal} + N_{jets} + N_{other} \quad (1)$$

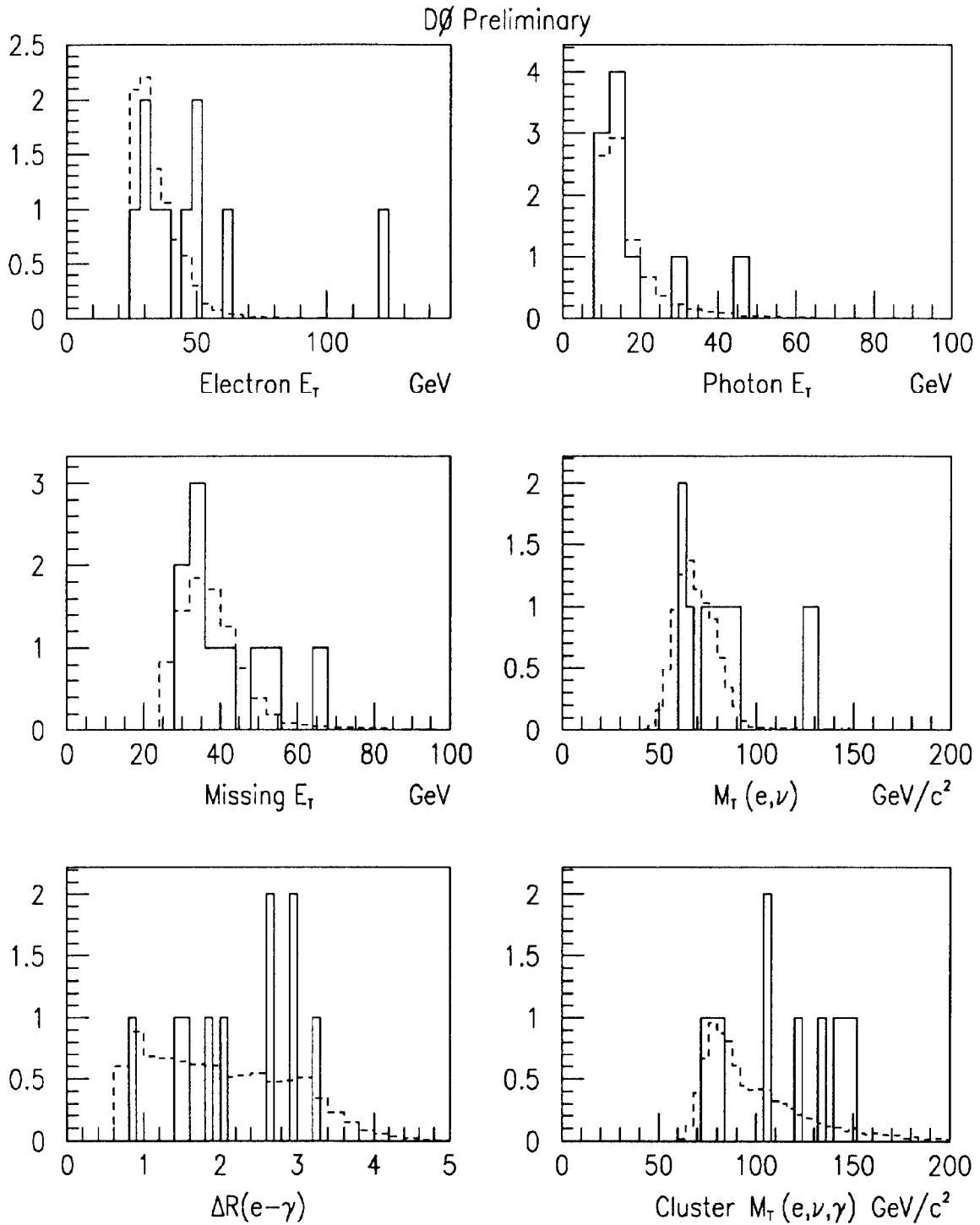


Figure 3: Distributions for the 10 $e\nu\gamma$ events. The solid lines are the data and the dashed lines are the Monte Carlo prediction.

DØ Preliminary

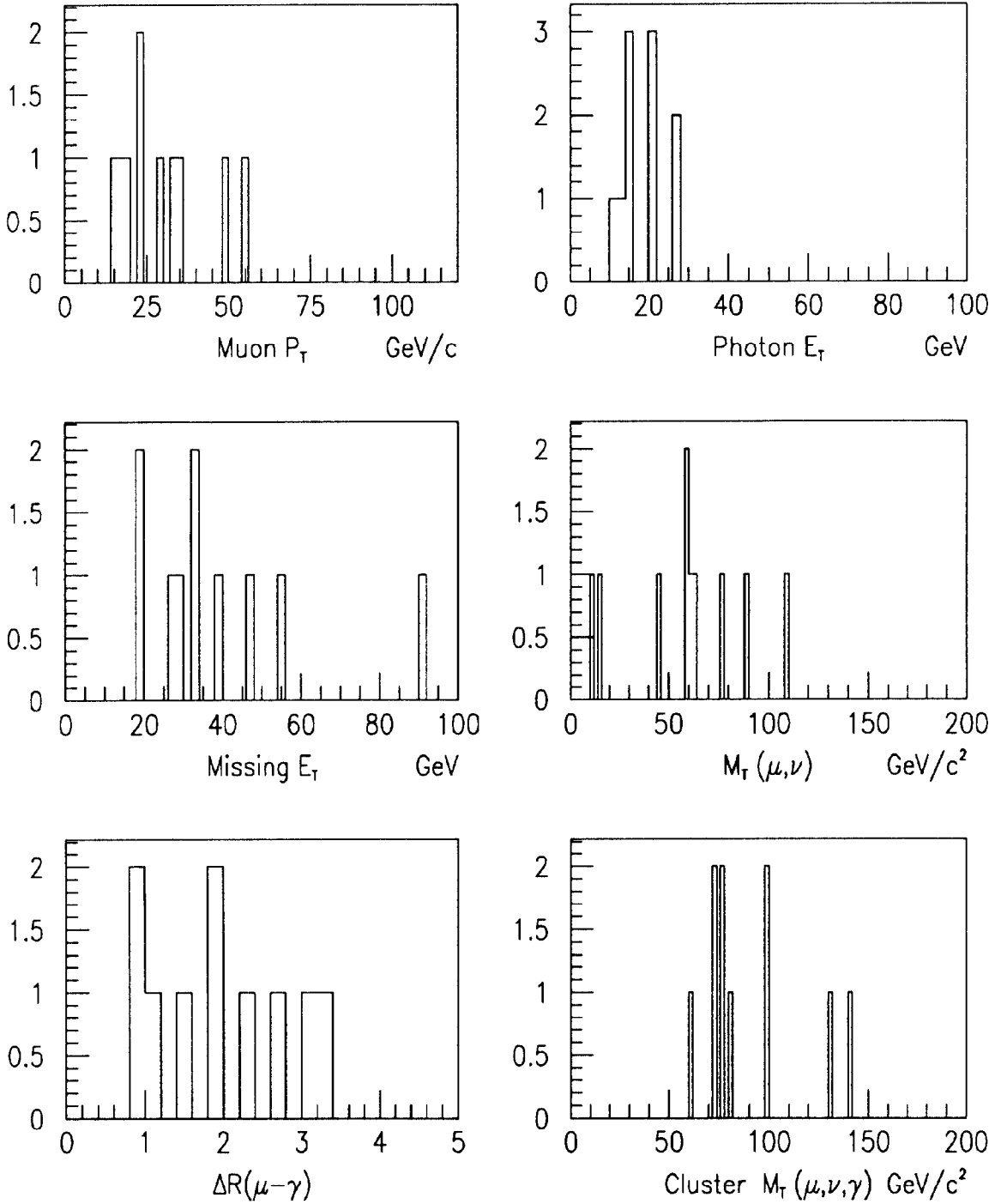


Figure 4: Distributions for the 10 $\mu\nu\gamma$ events.

where N_{other} represents either the $ee + \text{jets}$ (electron channel) or the cosmic ray (muon channel) backgrounds discussed below.

The proportionality factor for the second background ($Z\gamma + X$, where the Z decays to ee or $\mu\mu$ and one of the leptons is missed by the detector) is given by

$$f_Z = \frac{\sigma(Z\gamma)}{\sigma(W\gamma)} \times \frac{P(Z \rightarrow W_{acc})}{P(W \rightarrow W_{acc})}.$$

We estimate the cross section ratio using Monte Carlo generators of Baur and Zeppenfeld[9] using Standard Model couplings. The second factor is the ratio of Z and W decays that produce a lepton and \cancel{E}_T satisfying our kinematic and fiducial cuts; it is calculated using inclusive W and Z Monte Carlo samples. In the electron channel the resulting background factor is rather small: $f_Z(e) = 0.029 \pm 0.018$, while in the muon channel it is: $f_Z(\mu) = 0.25 \pm 0.05$.

The proportionality factor for the third background ($W\gamma$ with $W \rightarrow \tau\nu$ and $\tau \rightarrow l\nu\nu$) is calculated as

$$f_\tau = \frac{P(W_{\tau\nu} \rightarrow W_{acc})}{P(W_{l\nu} \rightarrow W_{acc})}.$$

The contribution from these cascade decays is suppressed both by the branching ratio $BR(\tau \rightarrow l\nu\nu = 0.18)$ and by the somewhat softer lepton momentum spectrum causing proportionally more to fail our E_T requirements. From a Monte Carlo calculation we obtain in the electron channel $f_\tau(e) = 0.019 \pm 0.002$ and in the muon channel $f_\tau(\mu) = 0.053 \pm 0.008$.

The fourth background (electron channel only) is any di-electron process (e.g. $Z \rightarrow ee$) where an electron is misidentified as a photon due to tracking inefficiency. To calculate this source of background we searched through our data sample for di-electron events that pass our event selection criteria and found 3 such events. The probability that an electron passes our photon criteria is determined by the tracking efficiency which is $(86.4 \pm 1.5)\%$ in the CC, and $(76.2 \pm 2.0)\%$ in the EC. Using these values, we calculate that this source of background contributes $N_{ee} = 0.4^{+0.7}_{-0.4}$ events.

The final background source considered is that from cosmic ray muons coincident with a $\bar{p}p$ collision that produces an event that satisfies our other selection criteria (i.e. a photon and \cancel{E}_T). Following the analysis of the inclusive $W \rightarrow \mu\nu$ [6], we estimate this contribution to be $N_{cosmic} = 0.0^{+0.9}_{-0.0}$ events.

Substituting the above values for the various sources of background in Eq. 1 we obtain the number of signal events:

<i>Electron Channel</i>	<i>Muon Channel</i>
$N_{\text{signal}} = 6.1 \pm 4.2 \text{ (stat)} \pm 1.8 \text{ (sys)}$	$N_{\text{signal}} = 6.0 \pm 4.2 \text{ (stat)} \pm_{-0.5}^{+1.0} \text{ (sys)}$

The statistical errors were calculated following the prescription for Poisson processes with background given in Ref. [8]. The contributions from the individual sources of background are summarized in Tables 1 and 2.

4. Acceptance and Efficiency

Using the above event selection procedures, the acceptance of the $D\bar{O}$ detector to the

Table 1. Electron Backgrounds

Source	N events
W + jets	3.2 ± 1.6
$Z\gamma$	0.18 ± 0.11
$W(\rightarrow \tau\nu)\gamma$	0.10 ± 0.01
$ee + jets$	$0.4^{+0.7}_{-0.4}$
Total bkgd	3.9 ± 1.8

Table 2. Muon Backgrounds

Source	N events
W + jets	1.5 ± 0.3
$Z\gamma$	2.1 ± 0.4
$W(\rightarrow \tau\nu)\gamma$	0.4 ± 0.1
Cosmics	$0.0^{+0.9}_{-0.0}$
Total bkgd	$4.0^{+1.0}_{-0.5}$

$\bar{p}p \rightarrow W\gamma + X$ events of interest was studied using the event generator of Baur and Zeppenfeld[9]. This program generates 4-vectors for $\bar{p}p \rightarrow W\gamma + X$ events for arbitrary $\Delta\kappa$ and λ , as described in Ref. [2]. These 4-vectors were then run through a fast detector simulation which smeared the electron, muon, photon, and missing transverse energies with the appropriate resolutions as determined from collider data. It also smeared the vertex position along the beam axis. The geometric acceptance of the fiducial volume used is approximately 52% (58%) in the electron (muon) channel for Standard Model couplings and increases by a few percent at the largest values of anomalous couplings considered here ($|\Delta\kappa| \leq 7.5, |\lambda| \leq 3$).

Efficiencies:

Triggering: In the electron channel, trigger turn-on curves for both the electron and the \cancel{E}_T requirement were determined from $D\bar{O}$ data samples, e.g. $Z \rightarrow ee$ or the inclusive W sample, and applied to the MC 4-vectors. These are very small effects given our analysis thresholds of 25 GeV.

In the muon channel the efficiency of the muon component of the trigger is $(73 \pm 5)\%$ in the central region (CF) and $(32 \pm 10)\%$ in the end region (EF). The photon component of trigger was determined to be $(95 \pm 5)\%$ efficient for our analysis threshold of 10 GeV.

Offline: The offline electron efficiency, including both tracking efficiency and the calorimeter requirements was found to $(79.2 \pm 1.8)\%$ in the CC and $(63.1 \pm 2.7)\%$ in the EC. The efficiency of muon reconstruction, as determined in the inclusive $W \rightarrow \mu\nu$ analysis, is $(46 \pm 5)\%$ in the CF and $(23 \pm 5)\%$ in the EF. The photon efficiency determination includes the losses due to photon conversion before the outermost tracking chambers as well as the effect of the calorimeter requirements (e.g. the χ^2 cut). The conversion losses (Fig. 5) were estimated by using a full GEANT

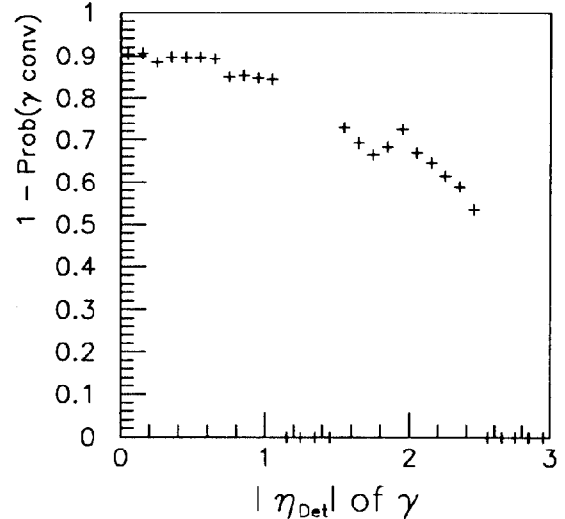


Figure 5: $1 - \text{Probability of a photon to convert as a function of detector pseudorapidity. The photon vertex is averaged over the } D\bar{O} \text{ luminous region.}$

simulation of the $D\bar{O}$ central detectors to calculate the number of radiation lengths of material encountered in each photon trajectory. We determined the efficiency of the calorimeter algorithm at high E_T using the response of electrons in the $Z \rightarrow ee$ and $W \rightarrow e\nu$ data samples. There is a gradual decrease of efficiency in the region below 20 GeV which we parameterized using test beam electrons. The loss of efficiency for photons due to an overlap with a random track was studied using inclusive W events and found to be negligible. In summary, the overall efficiency for Standard Model couplings is $(44 \pm 4)\%$ in the electron channel and $(17 \pm 3)\%$ in the muon channel.

5. Comparison with the Standard Model

Using the above efficiency and acceptance corrections, we can compare the observed signal with the predicted number of events for arbitrary values of the anomalous couplings. For the Standard Model couplings we expect in the electron channel $N_{pred}(e) = 8.7 \pm 0.9(\text{sys}) \pm 1.1(\text{lum})$ events. The first error is a (10%) systematic error arising from the uncertainty in our knowledge of the electron efficiency ($\pm 5\%$), the photon efficiency ($\pm 7\%$), and in our modelling of the \cancel{E}_T smearing in the fast detector simulation ($\pm 5\%$). The second error is a 12% uncertainty in the integrated luminosity. In the muon channel we expect $N_{pred}(\mu) = 6.9 \pm 1.0(\text{sys}) \pm 0.8(\text{lum})$.

In order to set limits on the anomalous couplings we calculate the expected number of events over a grid of values of $\Delta\kappa$ and λ and fit the results with a function that is quadratic in both couplings. For the electron channel, the expected number of events as a function of the couplings is shown in the upper two plots of Fig. 6 for $\lambda = 0$ and $\Delta\kappa = 0$, respectively. The central line of the parabola is the nominal expected value and the band indicates the $\pm 15\%$ systematic error in the prediction. The plot at the bottom of Fig. 6 shows the region excluded in the $\Delta\kappa$ - λ plane at $1\text{-}\sigma$ and $1.64\text{-}\sigma$ (one-sided 95% confidence level). Fig. 7 shows the analogous plots for the muon channel. Keeping one coupling fixed at the Standard Model value, we obtain single parameter limits (at the 95% confidence level) of:

<i>Electron Channel</i>	<i>Muon Channel</i>
$-2.7 \leq \Delta\kappa \leq 3.0 \ (\lambda = 0)$	$-3.9 \leq \Delta\kappa \leq 4.2 \ (\lambda = 0)$
$-1.3 \leq \lambda \leq 1.3 \ (\Delta\kappa = 0)$	$-1.7 \leq \lambda \leq 1.7 \ (\Delta\kappa = 0)$

We are able to combine these two results to produce improved limits by calculating the expected number of events, $N_{pred} = N_{pred}(e) + N_{pred}(\mu)$, for each point on the $\Delta\kappa \times \lambda$ grid and comparing this to the observed number of events: $N_{signal} = N_{signal}(e) + N_{signal}(\mu) = 12.1 \pm 5.9(\text{stat}) \pm_{1.9}^{2.1}$. The Standard Model prediction is $N_{pred} = 15.6 \pm 1.3(\text{eff}) \pm 1.9(\text{lum})$. From this procedure we obtain the results shown in Fig. 8 and the limits (at the 95% CL):

Combined Limits

$$\begin{aligned}
 -2.5 &\leq \Delta\kappa \leq 2.7 \ (\lambda = 0) \\
 -1.2 &\leq \lambda \leq 1.1 \ (\Delta\kappa = 0).
 \end{aligned}$$

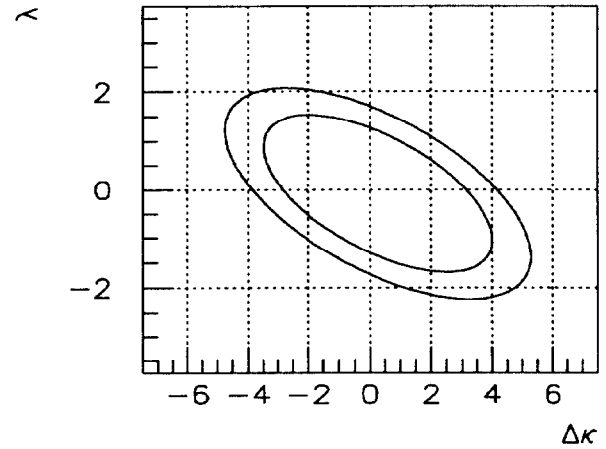
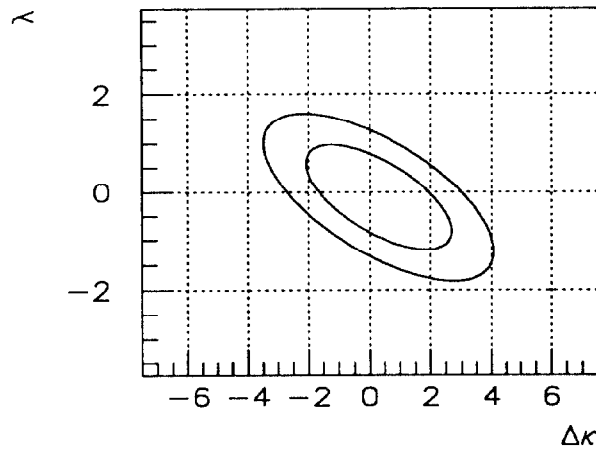
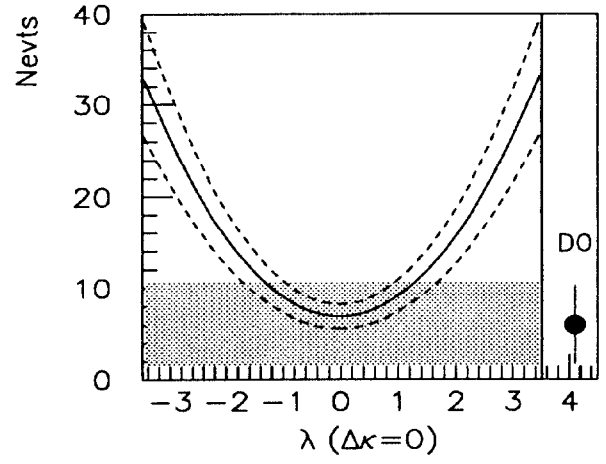
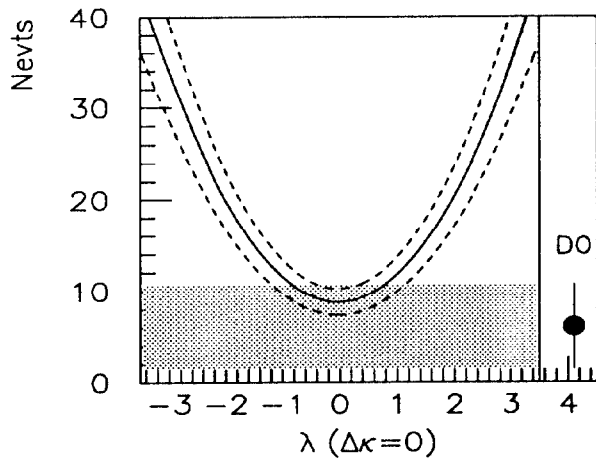
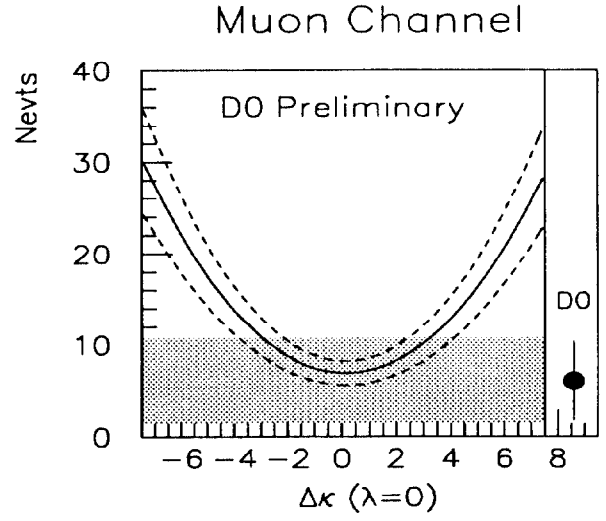
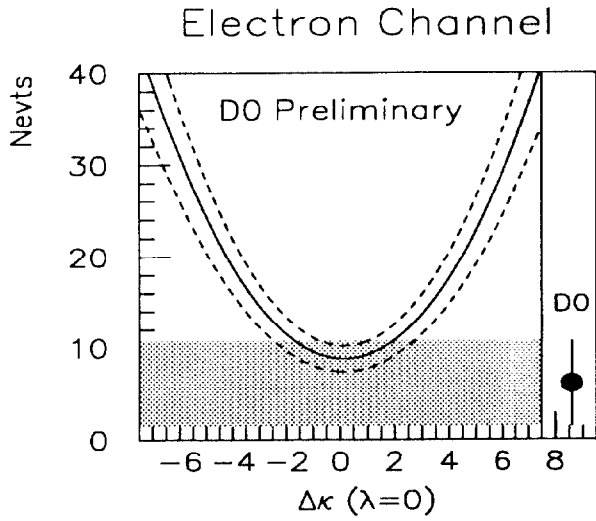


Figure 6: Number of expected events in the electron channel versus $\Delta\kappa$ (top) and λ (middle). The data point indicates N_{signal} . In the bottom plot the regions excluded at 1- σ and 95% CL are shown.

Figure 7: Number of expected events in the muon channel versus $\Delta\kappa$ (top) and λ (middle). The data point indicates N_{signal} . In the bottom plot the regions excluded at 1- σ and 95% CL are shown.

6. Conclusion

In conclusion, we have observed signals for the process $\bar{p}p \rightarrow W\gamma + X$ in the electron and muon channels in the data from the 1992/93 run at DØ. We have compared these observations with predicted values and set preliminary limits on anomalous $WW\gamma$ couplings. Analysis is in progress to improve on these limits by comparing the observed kinematic distributions with predictions. Furthermore, the upcoming run of the Fermilab collider is expected to provide about a factor of four larger data sample.

References

- [1] J. Cortès, *et al.*, Nucl. Phys. **B278**, 26, (1986)
- [2] U. Baur and E. L. Berger, Phys. Rev. D **41**, 1476 (1990)
- [3] W. Badgett, these Proceedings.
- [4] J. Alitti *et al.*, Phys. Lett. B **277**, 194 (1992)
- [5] S. Abachi *et al.*, FNAL-PUB-93/179, submitted to Nucl. Instrum. and Meth.
- [6] Norman Graf, these Proceedings.
- [7] DØ Collaboration (S. Abachi, *et al.*), Nucl. Instrum. Meth. **A324**, 53 (1993) and DØ Collaboration (H. Aihara, *et al.*), Nucl. Instrum. Meth. **A325**, 393 (1993)
- [8] Review of Particle Properties, Phys. Rev. D **45**, 1992. See Sec. 2.4.4
- [9] We are grateful to U. Baur for supplying us with the Monte Carlo routines used here as well as for helpful discussions.

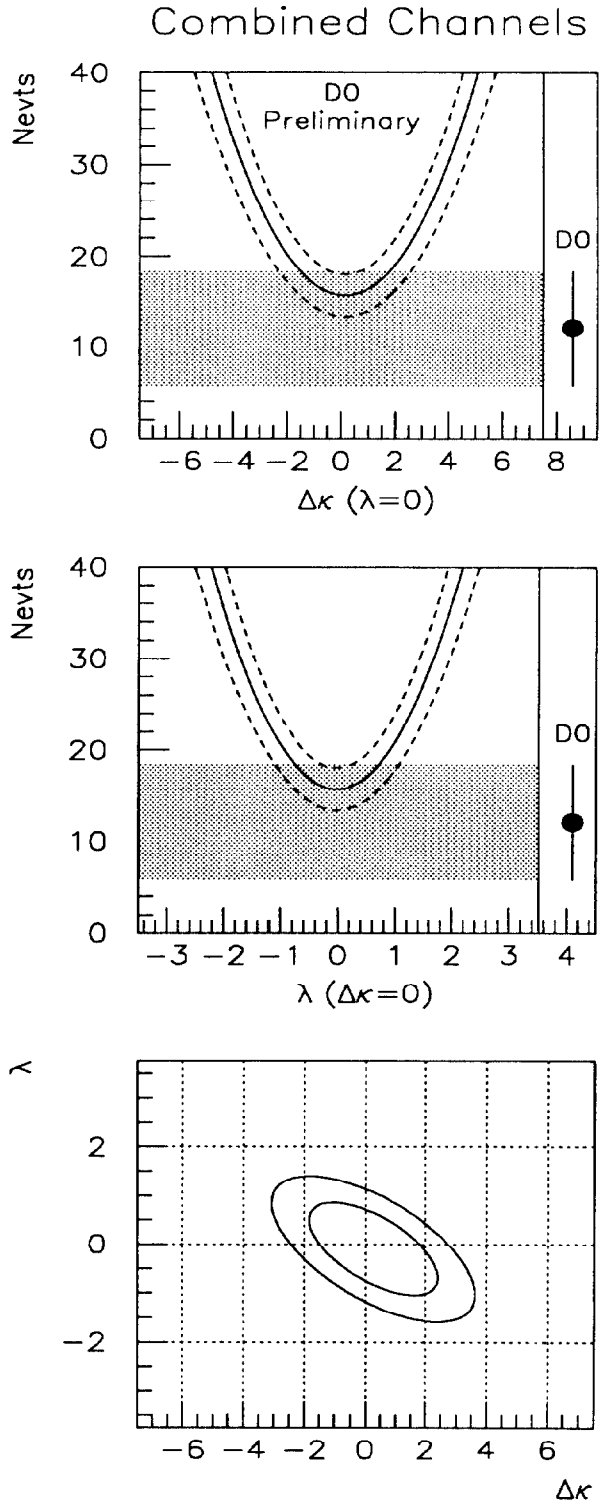


Figure 8: Number of expected events combining the electron and muon channels versus $\Delta\kappa$ (top) and λ (middle). The bottom plot shows the regions excluded at 1- σ and at 95% CL.